https://doi.org/10.2352/EI.2026.38.16.AVM-117

Circular-Edge SFR for Camera Image Quality Assessment: Theory, Implementation, and Validation

Xingbo Wang; Yanding Tech. Co., Ltd.; Shanghai, China
SangKyu Yang; CIZEN TECH Co., Ltd.; Gunpo, South Korea

Abstract

Traditional spatial frequency response (SFR) measurement, as defined by the ISO 12233 slanted-edge methodology, encounters significant measurement uncertainties and operational constraints when applied to wide-angle imaging systems. While recent updates to the standard incorporate polynomial edge-fitting to mitigate geometric warping, the underlying linear-edge model remains inherently limited by directional anisotropy and sampling phase instabilities at critical field angles. Furthermore, the rigid alignment requirements of slanted edges—often compromised by distortion-induced slope deviations—necessitate time-consuming mechanical orientation of the device under test (DUT) or the test target. This paper proposes a robust Circular-Edge SFR framework that synthesizes the broadband spectral coverage of the slanted-edge with the rotational invariance of the Siemens star. By employing a sub-pixel centroiding algorithm and a 60° tangent-aligned sector projection, the proposed method achieves continuous sampling phase integration and simultaneous extraction of SFR in any orientation, e.g., sagittal and tangential. Validation using synthetic equidistant projection models at a 100° field angle demonstrates that the circular-edge maintains high-fidelity measurements where traditional slanted edges collapse due to localized geometric stress. Notably, the superior azimuthal robustness and rotational symmetry of circles eliminate the 'critical angle' sampling failures. The framework provides a high-precision, alignment-independent solution for evaluating the image quality of wide-angle and fisheye camera systems.

Introduction

The assessment of Spatial Frequency Response (SFR)—serving as the measurable proxy for the Modulation Transfer Function (MTF)—is the cornerstone of modern camera metrology. For over two decades, the ISO 12233 slanted-edge methodology has been the industry benchmark, favored for its high signal-to-noise ratio (SNR) and its ability to derive a broadband spectral response from a compact Region of Interest (ROI).

However, the rapid evolution of imaging sectors, particularly in automotive sensing, autonomous robotics, and wide-field computer vision, has pushed traditional linear-edge models to their functional limits. These systems frequently employ wide-angle or fisheye optics characterized by extreme radial distortion. In such contexts, a physically linear edge is typically projected onto the image sensor as a curve—excepting the specific case of purely radial lines—thereby violating the rectilinear assumptions of the slanted-edge algorithm.

The literature reflects a diverse array of strategies to mitigate these geometric constraints, which can broadly be categorized into four classes: (1) pre-distorted test targets, which utilize compensated charts to appear rectilinear on-sensor but lack the versatility for general-purpose metrology [1]; (2) the Siemens star, which offers rotational symmetry but remains critically sensitive to distortion and center-localization errors in distorted fields [2]; (3) polynomial fitting, as seen in the ISO 12233:2023 update [2], which adapts the edge model to warped projections but fails to resolve sampling phase instabilities at critical 0°, 45° or 90° slant angles; and (4) circular-edge geometries, which have been explored for general SFR computation but often lack experimental validations regarding their performance in wide-field imaging systems [3].

Furthermore, the slanted-edge method is inherently anisotropic, capturing only the frequency response perpendicular to the edge transition. To characterize the full azimuthal variance—specifically the sagittal and tangential responses critical in wide-field image evaluation—multiple targets must be manually aligned at precise orientations. This requirement significantly increases chart complexity and introduces a high risk of mechanical alignment error or costly downtime during the calibration of the Device Under Test (DUT).

To address these limitations, this paper proposes a robust Circular-Edge SFR framework. Rather than "patching" the linear model, our approach leverages an integrated algorithmic pipeline that utilizes circular geometry to inherently align with any arbitrary direction of interest.

The remainder of this paper is structured as follows: Theoretical Analysis of Slanted-Edge Failure establishes the mathematical basis for measurement instability and sampling phase collapse in distorted fields. The Circular-Edge SFR Pipeline details our proposed methodology, from sub-pixel centroiding to tangent-aligned sector projection. Validation and Experiments provides a rigorous evaluation of the framework at a 100° field angle. Finally, Results, Discussion, and Conclusion presents a comparative analysis of the results, discussing performance consistency and angular robustness, and concludes with a summary of future research directions.

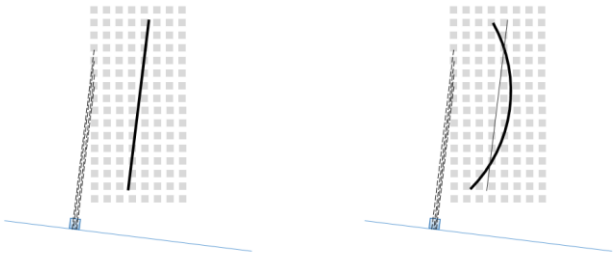

***Figure 1**. Comparison of spatial binning consistency and its impact on the Edge Spread Function (ESF). (Left) In a rectilinear system, linear projection correctly aggregates pixels with identical geometrical distances from the edge manifold, ensuring each sub-pixel bin captures a coherent phase. (Right) Radial distortion introduces a coordinate mismatch where the straight-line assumption fails to follow the curved manifold. Pixels at disparate true geometrical distances are erroneously aggregated into shared bins, artificially blurring the edge and degrades the reported SFR.*

Theoretical Analysis of Slanted-Edge Failure

The mathematical integrity of the ISO 12233 slanted-edge method is predicated on the assumption that the edge within a selected Region of Interest (ROI) is perfectly linear. When this assumption is met, the algorithm successfully constructs an oversampled Edge Spread Function (ESF) by sorting pixels into sub-pixel bins based on their perpendicular distance to the edge. However, in systems characterized by significant radial distortion, this rectilinear model collapses.

The first mode of failure is a geometric mismatch that leads to a loss of bin-coherence. Because the algorithm projects two-dimensional pixel coordinates onto a one-dimensional linear axis, it fails to account for the physical curvature of the distorted edge manifold. Consequently, pixels that reside at different true geometrical distances from the curved edge are mathematically forced into the same spatial bin. This projection error introduces extra blurs to the image and widens ESF.

***Figure 2**. Distortion-induced transformation of edge orientation. (Left) Standard 5° slant providing uniform sub-pixel sampling. (Middle) Radial rotation toward 0° inducing phase collapse and a staircase ESF. (Right) An effectively 22° edge leading to oversampling rate shifts and orientation-dependent measurement bias.*

Beyond this geometric misalignment, a second failure mode emerges regarding the stability of the sampling phase. A reliable SFR measurement requires a diverse distribution of sub-pixel phases to accurately reconstruct the transition from dark to light. In standard conditions, a slant angle of approximately 5.7° ensures that the edge "drifts" across the pixel grid at a rate of one-tenth of a pixel per row, providing a uniform sampling distribution. However, as illustrated in Fig. 2, radial distortion actively rotates the local orientation of the target relative to the sensor's pixel grid.

A target designed at a compliant 5.7° slant may be warped into an effectively 0°, 45° or 90° edge, triggering a phase collapse. In this state, every pixel in a given row or column bears the exact same spatial relationship to the edge, leading to exactly the same ESF in each row or column. Conversely, in other cases, the same target may be stretched into an effectively 22° edge. This rotation fundamentally shifts the oversampling rate from the intended 10× to approximately 2.5×, while simultaneously introducing orientation-dependent bias, as the MTF of lenses and pixels are typically non-isotropic.

The Circular-Edge SFR Pipeline

The proposed pipeline replaces the linear projection of the ISO 12233 standard with a radial framework (see Fig. 3). By utilizing the inherent symmetry of a circular target, the algorithm remains invariant to the rotational effects of radial distortion, providing a consistent metric across the entire field of view.

Phase 1: ROI Initialization and Preprocessing

The initial phase prepares the raw sensor data for geometric analysis by ensuring intensity linearity and spatial isolation.

Step 1: ROI Selection and Linearization: The user specifies a Region of Interest (ROI) containing the circular test target. If the source is a color image, it is converted to a grayscale image by calculating Luminance (Y) at each pixel. Crucially, the data undergoes linearization to reverse any applied gamma correction or OETF. This ensures that pixel intensity values are directly

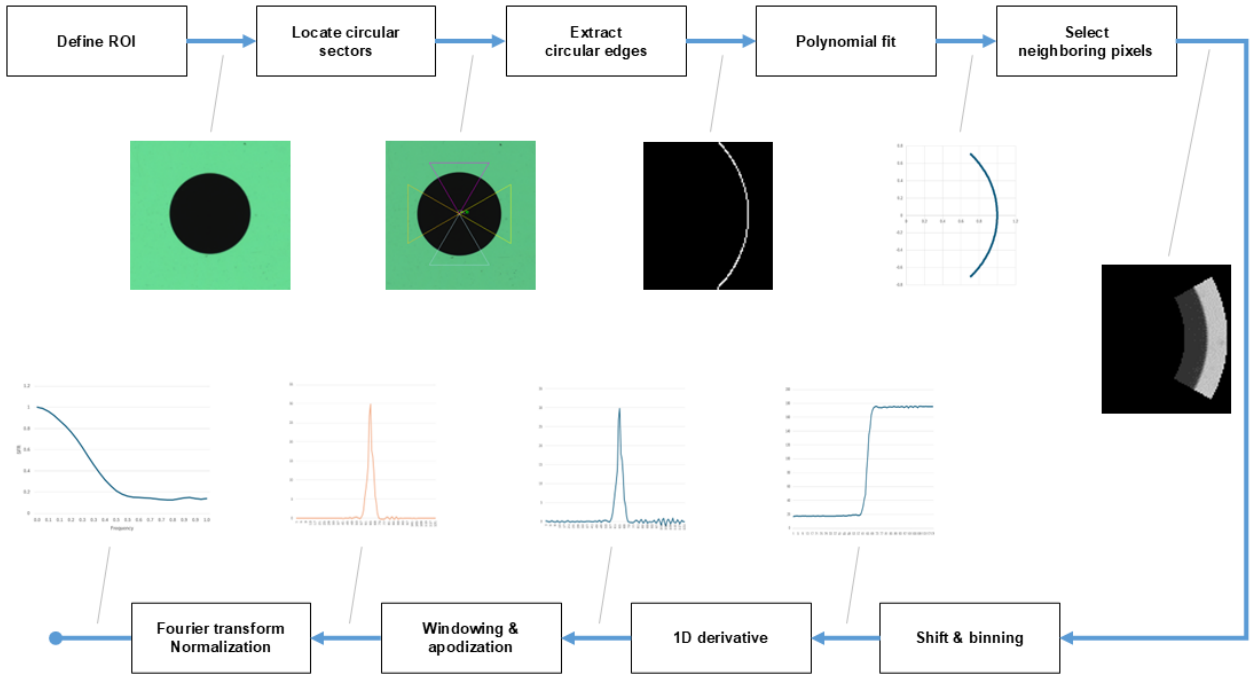

***Figure 3.** The circular edge SFR pipeline*

proportional to scene radiance, preventing "gamma smearing" from biasing the MTF calculation.

Step 2: Center Localization and Sector Specification: An initial sub-pixel center (x0, y0) is estimated with sub-pixel accuracy. Following this, the user manually defines the angular orientation and span ($\Delta\theta = 60°$ in this paper) of the circular sectors. This allows the researcher to isolate specific radial zones—such as tangential or sagittal regions—to characterize asymmetric optical performance. Unlike the slanted-edge, which is locked into its printed orientation, this circular sector integrates a range of infinitesimal tangents within the user's chosen window, providing a robust "mean" SFR for that specific orientation.

Step 3: Edge Detection: An edge detector is applied within the ROI to extract the coordinates of the arc manifold. The resulting coordinates serve as the foundational data for all subsequent geometric modeling.

Phase 2: Geometric Manifold Fitting

This phase creates the mathematical "anchor" that describes how the lens has warped the target.

Step 4: Polynomial Edge Fitting: Using the detected edge coordinates and the estimated center, a polynomial fit $R(\theta)$ is performed. This function describes the radius of the edge as a function of the polar angle θ. By allowing the radius to vary with θ, the model accounts for imperfect circularity, centration errors, and high-order distortion at the field periphery.

Phase 3: Radial Coordinate Mapping

This is the core "fix" for the geometric failures identified in the preceding section, transforming a 2D warped image into a 1D signal.

Step 5: Geometrical Distance Calculation: For every pixel Pi at (xi, yi) within the sector, the algorithm calculates its exact geometrical distance di from the fitted manifold:

$$d_i = \sqrt{(x_i - x_0)^2 + (y_i - y_0)^2} - R(\theta_i) \quad (1)$$

This transformation effectively "flattens" the 2D curved manifold into a 1D distance vector. This ensures that pixels are binned according to their true geometrical transition phase, completely eliminating the issues resulting from linear projection.

Phase 4: SFR Computation

The final phase converts the spatially corrected radial data into the frequency domain.

Step 6: Super-sampled ESF Construction: Pixels are sorted by their distance di into 0.25-pixel bins. This creates a high-density ESF. Because the circular edge naturally provides a continuous distribution of phases along its arc, this ESF avoids the insufficient samples often seen in near-vertical slanted edges.

Step 7: LSF Derivation: The Line Spread Function (LSF) is computed via the first-order derivative of the ESF. This represents the system's impulse response along the radial axis.

Step 8: Conditioning (Hamming and Apodization): A Hamming window is applied to the LSF to truncate the signal gracefully. This reduces spectral leakage and the impact of sensor noise in the dark/light regions of the ROI, which can otherwise "inflate" the MTF at high frequencies.

Step 9: DFT and SFR Calculation: A Discrete Fourier Transform (DFT) is applied to the conditioned LSF. The resulting magnitude spectrum is normalized to DC (zero frequency), yielding the final Spatial Frequency Response (SFR).

Validation and Experiments

The primary challenge in validating SFR algorithms in practice is the absence of ground truth; in physical captures, the "true" SFR is invariably confounded by sensor crosstalk, non-uniform illumination, and noise. To isolate the algorithmic precision of the Circular-Edge pipeline, we utilized a synthetic simulation framework where the ground truth is mathematically defined.

Simulation Framework and Projection Models

The validation workflow begins with the generation of idealized, infinitely sharp slanted-edge and circular-edge patterns. We then simulate two distinct optical environments, i.e., the Rectilinear Projection Baseline—an ideal pinhole system, representing zero distortion—and the Equidistant Projection—a camera of an angular field of view of 100°. As the field angle increases, the disparity between these models becomes severe, with the equidistant model introducing significant radial compression/stretching compared to the rectilinear ideal.

Isolation of Geometric Variables

To ensure a rigorous comparison, we incorporated two fundamental blurring components: lens diffraction (Airy pattern) and square-shaped pixel aperture geometry.

In an aberration-free, diffraction-limited system, the Point Spread Function (PSF) is determined by the diffraction of a circular exit pupil, resulting in the characteristic Airy pattern. The normalized Airy intensity distribution I(r) as a function of the radial distance r from the optical axis is given by:

$$I(r) = \left[\frac{2J_1(\pi r/\lambda N)}{\pi r/\lambda N}\right]^2 \quad (2)$$

where J1 is the first-order Bessel function of the first kind, λ is the wavelength, and N is the f-number of the lens.

The second component of the blur is the "Pixel Geometry PSF". We model the sensor using square pixels of width w. The process of a pixel collecting photons over its surface area is mathematically equivalent to a 2D Box (Rect) convolution followed by discrete sampling. The spatial response h(x,y) is defined as:

$$h(x,y) = rect\left(\frac{x}{w}\right) rect\left(\frac{y}{w}\right) \quad (3)$$

The combined PSF serves as the absolute benchmark for our validation. By applying the combined convolution kernel to all images, we ensured that distortion is independent of blurring, and any variance in the resulting SFR between any pair of results can be attributed solely to the SFR algorithm.

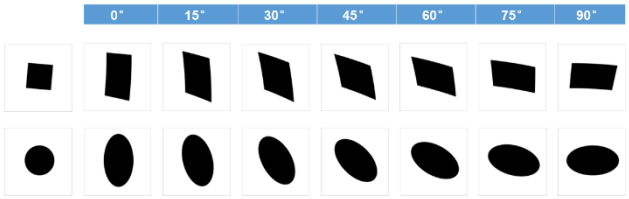

Figure 4*. Synthetic test target series generated for azimuthal sensitivity analysis (0◦ to 90◦ at 15◦ intervals). Both the traditional slanted-square (top) and proposed circular-edge (bottom) targets were mapped using an equidistant projection model to simulate 100◦ wide-angle distortion. A constant blurring kernel, incorporating the Airy pattern and pixel geometry PSF, was applied to both series to isolate geometric projection error from blurring.*

Azimuthal Sensitivity Analysis

Recognizing that the influence of distortion varies significantly with the azimuth, we analyzed the targets across a comprehensive range of orientations—from 0° to 90° at 15° intervals. To maintain consistency with industry tradition, we focused our validation on the horizontal and vertical SFR performance. This process yielded two distinct series of distorted edges (see Fig. 4).

Results, Discussion and Conclusion

The first stage of validation compared the slanted-edge and circular-edge SFRs in a zero-distortion (rectilinear) environment. As can been seen from Fig. 5, both methods yielded nearly identical results, maintaining high consistency up to the Nyquist frequency. This confirms that the circular-edge pipeline is fundamentally sound.

The second stage compared the two methods under 100° equidistant distortion, using the undistorted slanted-edge SFR as a reference. Despite the severe geometric warping shown in Fig. 4, the circular-edge SFR remained remarkably consistent with the undistorted reference. This demonstrates that the radial framework successfully neutralizes the equidistant projection error.

The circular-edge SFR framework addresses ISO 12233's geometric failures in wide-angle image evaluation. By employing radial coordinate mapping, the pipeline remains invariant to equidistant distortion. Results confirm that circular-edge SFR is highly consistent with slanted-edge methods while overcoming critical-angle limitations and providing superior rotational symmetry for directional versatility.

Future work will investigate specific slanted-edge failure modes and minor numerical discrepancies between these methods in detail to quantify the absolute accuracy gains of the circular approach.

References

[1] N. Koren, "The Imatest program: Comparing cameras with different amounts of sharpening," in Electronic Imaging 2006: Digital Photography II, San Jose, California, United States, 2006

[2] Photography — Electronic still picture imaging — Resolution and spatial frequency responses, ISO Standard 12233:2023, 2023.

[3] R. L. Baer, "The circular-edge spatial frequency response test," in Electronic Imaging 2004: Image Quality and System Performance, San Jose, California, United States, 2003.

Acknowledgement

Special thanks to Mr. Chanki Jung of CIZEN TECH for his programming efforts and contributions to the technical discussions.

Author Biography

Xingbo Wang received an MSc from the Erasmus Mundus programme in color in informatics and media technology (2011) and a subsequent PhD in computer science from the Norwegian University of Science and Technology (2016). Driven by a lifelong fascination with camera fundamentals, he currently serves as an image scientist with Yanding. His professional research focuses on the rigorous imaging performance analysis of digital cameras for both photographic and automotive use. He also actively participates in ISO and IEEE standardization efforts.

SangKyu Yang received his master's degree in Information and Communication Engineering from MyongJi University. Previously at isMedia, he developed compact camera module active alignment and focus test equipment. Currently, he is the founder of CIZEN TECH, where he leads the development of MTF and distortion evaluation systems. He specializes in the advancement of high-precision measurement and calibration technologies for automotive imaging applications.

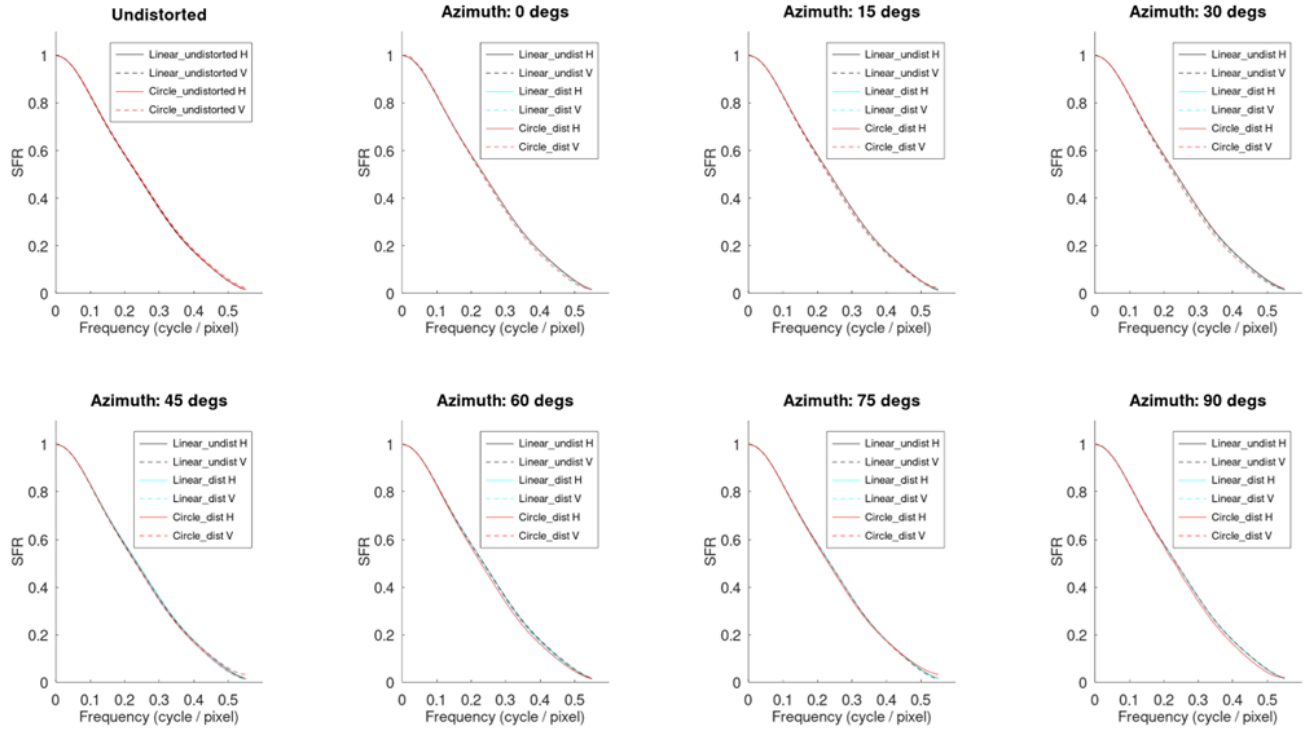

***Figure 5**. Comparative SFR analysis of slanted-edge and circular-edge targets*

JOIN US AT THE NEXT EI!

electronic IMAGING

Imaging across applications . . . Where industry and academia meet!

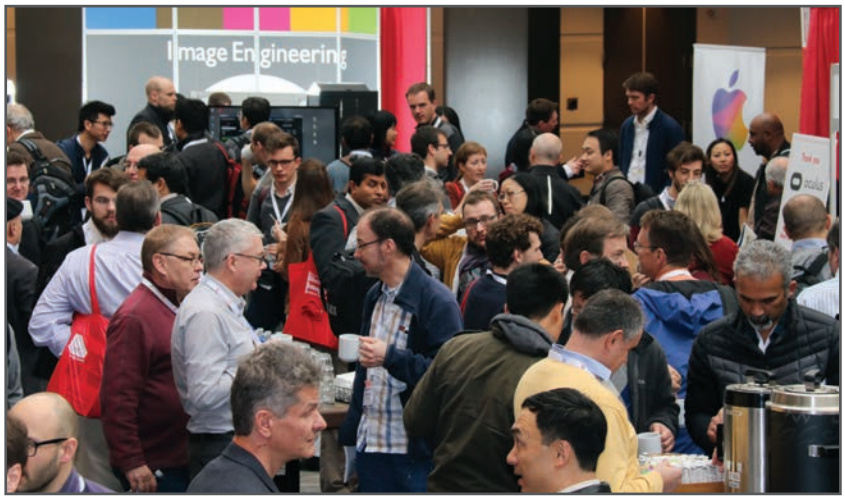

• SHORT COURSES • EXHIBITS • DEMONSTRATION SESSION • PLENARY TALKS •
• INTERACTIVE PAPER SESSION • SPECIAL EVENTS • TECHNICAL SESSIONS •

www.electronicimaging.org

ADVANCING IMAGING SCIENCE 75 1947 IS&T 2022 imaging.org